Plant Molecular Biology (2019) 101:325–339
https://doi.org/10.1007/s11103-019-00908-9

Proteomic characterization of MPK4 signaling network and putative substrates

Tong Zhang[1,6] · Shweta Chhajed[1] · Jacqueline D. Schneider[1] · Guanqiao Feng[2] · Wen-Yuan Song[2,3,4] · Sixue Chen[1,2,4,5]

Received: 2 April 2019 / Accepted: 6 August 2019 / Published online: 9 August 2019

Key message **Combining genetic engineering of MPK4 activity and quantitative proteomics, we established an *in planta* system that enables rapid study of MPK4 signaling networks and potential substrate proteins.**

Abstract Mitogen activated protein kinase 4 (MPK4) is a multifunctional kinase that regulates various signaling events in plant defense, growth, light response and cytokinesis. The question of how a single protein modulates many distinct processes has spurred extensive research into the physiological outcomes resulting from genetic perturbation of *MPK4*. However, the mechanism by which MPK4 functions is still poorly understood due to limited data on the MPK4 networks including substrate proteins and downstream pathways. Here we introduce an experimental system that combines genetic engineering of kinase activity and quantitative proteomics to rapidly study the signaling networks of MPK4. First, we transiently expressed a constitutively active ($MPK4^{CA}$) and an inactive ($MPK4^{IN}$) version of a *Brassica napus* MPK4 (*Bn*MPK4) in *Nicotiana benthamiana* leaves. Proteomics analysis revealed that *Bn*MPK4 activation affects multiple pathways (e.g., metabolism, redox regulation, jasmonic acid biosynthesis and stress responses). Furthermore, *Bn*MPK4 activation also increased protein phosphorylation in the phosphoproteome, from which putative MPK4 substrates were identified. Using protein kinase assay, we validated that a transcription factor TCP8-like (TCP8) and a PP2A regulatory subunit TAP46-like (TAP46) were indeed phosphorylated by *Bn*MPK4. Taken together, we demonstrated the utility of proteomics and phosphoproteomics in elucidating kinase signaling networks and in identification of downstream substrates.

Keywords MPK4 · Proteomics · Phosphoproteomics · Kinase network · Substrate

Introduction

Plants constantly respond to various biotic and abiotic environmental stimuli. To enable rapid cell signaling, reversible protein phosphorylation and dephosphorylation emerged as universal post-translational modifications (PTMs) in essentially all aspects of plant life (Zhang et al. 2014, 2018a; Mithoe and Menke 2018). This is highlighted by the remarkable evolutionary expansion of plant protein kinases (PKs), the enzymes that catalyze the transfer of a phosphate group from ATP to specific protein substrates. For example, 4% of protein-coding genes in the *Arabidopsis* genome encode PKs, comparing to 2% in the human genome (Zulawski et al. 2014). Among various plant PKs, mitogen-activated PKs (MPKs) relay environmental and developmental cues through phosphorylation of downstream signaling proteins (Pitzschke et al. 2009a; Xu and Zhang 2015). A distinct feature of MPK-mediated signaling is that three tiers of PKs form a sequential phosphorylation cascade, consisting of

Electronic supplementary material The online version of this article (https://doi.org/10.1007/s11103-019-00908-9) contains supplementary material, which is available to authorized users.

✉ Sixue Chen
schen@ufl.edu

1 Department of Biology, University of Florida, Gainesville, FL 32611, USA

2 Plant Molecular and Cellular Biology Program, University of Florida, Gainesville, FL 32610, USA

3 Department of Plant Pathology, University of Florida, Gainesville, FL 32611, USA

4 Genetics Institute, University of Florida, Gainesville, FL 32610, USA

5 Proteomics and Mass Spectrometry, Interdisciplinary Center for Biotechnology Research, University of Florida, Gainesville, FL 32610, USA

6 Present Address: Biological Sciences Division, Pacific Northwest National Lab, Richland, WA 99354, USA

MPK, MPK kinase (MPKK), and MPKK kinase (MPKKK). These PKs (with 60 MPKKKs, 20 MPKKs and 10 MPKs in the reference plant *Arabidopsis*) are organized into different pathways to cope with a diverse array of external signals (MAPK Group 2002; Hamel et al. 2012). As the terminal player of the cascade, MPKs interact with specific downstream proteins to trigger proper cellular responses (Pitzschke 2015; Zhang et al. 2016). A growing body of evidence suggests the multiple functional nature of MPKs, as exemplified by MPK4 with diverse functions in growth and development (Petersen et al. 2000), plant immunity (Wang et al. 2009), response to abiotic stress (Droillard et al. 2004), cytokinesis (Kosetsu et al. 2010) and recently in light signaling (Li et al. 2016). Notwithstanding the rich information on the diverse roles that MPKs play, few substrate proteins have been identified to date. Thus, identifying MPK networks and responsive cellular pathways is a prerequisite for mechanistic understanding of the MPK signaling cascades.

Previous studies have relied on traditional approaches such as yeast two-hybrid (Andreasson et al. 2005; Zhao et al. 2005; Singh et al. 2012; Xie et al. 2012) to identify potential MPK substrates. The yeast two-hybrid system pushes interactions to occur in the nucleus, and is known to produce false positive results. In addition, incorrect folding and PTMs of plant proteins in yeast may also contribute to false negative results. Protein/peptide arrays, based on the interactions between kinases and potential substrates, have also been used in the identification of potential kinase substrates (Feilner et al. 2005; Popescu et al. 2009). To study the molecular pathways regulated by MPKs, transcriptomics has been applied to compare the global gene expression profile between wild type and *MPK* overexpression/knockout plants (Petersen et al. 2000; Brodersen et al. 2006; Brader et al. 2007; Singh et al. 2012; Katou et al. 2013). This systems biology approach has revealed multiple MPKs-modulated processes including differentiation, response to biotic (bacterial and fungal infection) and abiotic stresses (e.g. wounding, temperature, light and ozone). However, the dynamic protein changes and actual effectors in biological processes have not been fully explored. More importantly, MPKs function through phosphorylation, the information of which cannot be gleaned or deduced from transcriptomic analysis. In contrast, proteomics has shown utility in characterizing not only the pathways downstream of kinase activation, but also key PTM events in signaling transduction that are not amenable to other approaches (Li et al. 2015; Balmant et al. 2016; Furlan et al. 2017; Zhu et al. 2017; Ma et al. 2018). Application of phosphoproteomics has yielded successful identification of putative substrates of MPK3/6 (Hoehenwarter et al. 2013; Lassowskat et al. 2014; Rayapuram et al. 2018), and SnRK2 (Umezawa et al. 2013; Wang et al. 2013).

Here we designed a proteomics approach with the aim to profile cellular pathways responsive to the activation of MPKs and to identify potential MPK substrates. We have biochemically characterized *Brassica napus* MPK4 as an active kinase with both auto-phosphorylation and trans-phosphorylation activities (Zhang et al. 2015), and thus used it as a model in this study. To rapidly assess gene functions *in planta*, we transiently expressed a constitutive active *Bn*MPK4 (MPK4^{CA}) and an inactive variant of *Bn*MPK4 (MPK4^{IN}) in *Nicotiana benthamiana* leaves. Transient expression in *N. benthamiana* has been widely used in plant science, producing protein of interests *in planta* within 2 to 3 days (Goodin et al. 2008; Leuzinger et al. 2013; Norkunas et al. 2018; Qi et al. 2018; Wang et al. 2018). Due to its simple experimental procedure and transient expression *in planta*, this method is well-suited to study cellular signaling components such as PKs (Zipfel et al. 2006; Takahashi et al. 2007; Asai et al. 2013; Cheng et al. 2013; Wang et al. 2015; Yamada et al. 2016).

An isobaric tandem mass tags (TMTs)-based quantitative proteomics was performed to compare global protein abundances between the *Bn*MPK4^{CA}- and *Bn*MPK4^{IN}-expressing *N. benthamiana* leaves. Differential proteome analysis showed that MPK4 activation results in profound changes in biological pathways such as signaling transduction, responses to stress and growth. In addition, distinct phosphorylation patterns were observed following *Bn*MPK4 activation, which allowed the identification of a list of 71 putative MPK4 substrates. We also used kinase activity assay to provide orthogonal validation that a transcription factor (TF) TCP8-like (TCP8) and a PP2A regulatory subunit TAP46-like (TAP46) can indeed be phosphorylated by the *Bn*MPK4.

Materials and methods

Plant materials

Nicotiana benthamiana seedlings were germinated in a Metro-Mix 500 potting mixture (The Scotts Co.), and grown in a growth chamber at 24 °C under a 16/8 h light/dark cycle. Five-week old plants were used to transiently express the *BnMPK4^{CA}* and *BnMPK4^{IN}* under a cauliflower mosaic virus (CaMV) 35S promoter. Mutagenesis for creating the active and inactive MPK4s has been described previously (Berriri et al. 2012; Zhang et al. 2015). Construction of the vectors for protein expression, transformation of *Agrobacterium tumefaciens* strain C58C1, and infiltration of plant leaves had been described previously (Huang et al. 2013; Zhang et al. 2015).

In-gel kinase assay

To determine the kinase activity of *Bn*MPK4s expressed in *N. benthamiana* leaves, samples were collected at 2 days after infiltration. Protein was extracted in 50 mM Tris–HCl, pH 7.4, 150 mM NaCl, 1 mM EDTA, 1% Triton X-100 containing protease and phosphatase inhibitor cocktails (Thermo Scientific, Rockford, IL, USA), and the crude extracts were subjected to in-gel kinase assay as described previous (Zhang et al. 2015).

Sample preparation for TMT-based quantitative proteomics

Proteins were extracted from the infiltrated *N. benthamiana* leaves by a phenol method as described previously (Zhang et al. 2017, 2018b). This study consisted of TMT labeling and quantification of six biological samples, each from an individual plant. They are three biological replicates of *Bn*MPK4^{CA} labeled with TMT tags 126, 127 and 128, and three biological replicates of *Bn*MPK4^{IN} labeled with TMT tags 129, 130 and 131. Briefly, 0.2 g of each sample was ground into fine powder in liquid nitrogen using a pestle and mortar. The powder was re-suspended in equal volumes of Tris-buffered phenol (pH 8.8) and extraction buffer (0.1 M Tris–HCl, pH 8.8, 10 mM EDTA, 0.4% β-mercaptoethanol and 0.9 M sucrose with protease and phosphatase inhibitor cocktail, Thermo Scientific). After 1 h shaking at room temperature, the samples were centrifuged at 20,000 × g for 30 min at 4 °C. The top phenol phase was transferred into a new tube, and the proteins were precipitated overnight in 0.1 M ammonium acetate in 100% methanol. The pellets were washed twice in 80% acetone and once in 100% acetone. The pellets were dissolved in 8 M urea, 25 mM triethyl ammonium bicarbonate (TEAB), 0.05% sodium dodecyl sulfate (SDS), and 1% Triton X-100. Protein concentrations were measured using an EZQ quantification kit (Thermo Scientific). Protein samples were diluted 7-fold with 100 mM TEAB, reduced by 10 mM Tris (2-carboxyethyl) phosphine at 37 °C for 1 h, followed by alkylation with 20 mM iodoacetamide in the dark for 30 min. Trypsin (Promega) in 100 mM TEAB was added to the protein samples (enzyme:sample = 1:100 w/w) for overnight digestion at 37 °C. The digested peptides were desalted by MacroSpin Column Silica C_{18} columns (The Nest Group), and then labeled with a TMT-6pex kit (Thermo Scientific) according to the manufacturer's instructions. The labeling was quenched by adding 5% hydroxylamine to the reaction mixture, and the samples were subsequently pooled.

The TMT labeled samples were fractionated on a PolySULFOETHYL A column (100 × 2.1 mm, 5 µM, 300 Å) using strong cation exchange liquid chromatography (LC) with a low salt buffer A [25% acetonitrile (ACN), 10 mM ammonium formate, 0.1% formic acid, pH 2.8] and a high-salt buffer B (25% ACN, 500 mM ammonium formate, pH 6.8) as mobile phases. The flow rate was set at 0.2 mL/min with the following gradient: 0–10 min: 100% A; 10–90 min: 80% A and 20% B; 90–95 min: 100% B. Thirty-eight fractions were collected, and then combined into six fractions. Each fraction was desalted, and 5% was aliquoted for global proteome analysis. The remaining 95% of each fraction was subjected to phosphopeptide enrichment. Briefly, the peptides were resuspended in 40 µL of the sample solution (3% ACN, 0.1% acetic acid, 0.01% trifluoroacetic acid) and 40 µL of the binding solution (80% ACN, 5% TFA), and then loaded on to a NuTip minicolumn ($TiO_2 + ZrO_2$, Glygen, Columbia, MD, USA). After washing with 80% CAN (acidified with 1% TFA), the enriched peptides were eluted with 3% ammonium hydroxide and speed-vac dried.

Nanoflow liquid chromatography–tandem mass spectrometry (nanoLC–MS)

Peptides derived from the total protein digests and phosphopeptide-enriched samples were resuspended in 0.1% formic acid for nano-LC–MS analysis. The bottom-up proteomics data acquisition was performed on an EASY-nLC 1000 liquid chromatography system (Thermo Scientific) connected to an Orbitrap Fusion Tribrid instrument equipped with a nano-electrospray source (Thermo Scientific). Samples were loaded onto an Acclaim PepMap® 100 C_{18} trapping column (75 µm i.d. × 2 cm, 3 µm, 100 Å) and then separated on a PepMap® C_{18} analytical column (75 µm i.d. × 25 cm, 2 µm, 100 Å). The flow rate was set at 300 nL/min with solvent A (0.1% formic acid in water) and solvent B (0.1% formic acid in ACN) as the mobile phases. Separation was conducted using the following gradient: 5–7% of B over 0–5 min, 7–25% of B over 5–105 min, 25–60% of B over 105–115 min, 60–95% of B over 115–120 min and isocratic at 95% of B over 120–130 min.

For MS data acquisition, the full MS1 scan (m/z 380–1500) was performed in the high field Orbitrap with a resolution of 120,000 at m/z 400. The automatic gain control (AGC) target was 2e5 with 50 ms as the maximum injection time. Monoisotopic precursor selection (MIPS) was enforced to filter for peptides. Peptides bearing 2–6 charges were selected for fragmentation with an intensity threshold of 5e3. Dynamic exclusion of 45 s was used to prevent resampling high abundance peptides. Top speed method was used for data dependent acquisition within a cycle of 3 s. Four scan events were set for peptides with + 2, + 3, + 4, and + 5 to + 6 charges, respectively. Scan event one comprised an isolation of doubly charged peptides with an isolation window of 0.7 Da in the quadrupole mass analyzer, fragmentation of the selected peptides by collision induced dissociation (35% of normalized collision energy). The MS2 spectra were

detected in the linear ion trap with the AGC target of 1e4 and a maximum injection time of 50 ms. Multi-notch isolation of MS2 spectra were performed in the ion trap with a 0.7 Da window, and the selected ions were further dissociated by higher-energy collisional dissociation (HCD, 65% of normalized collision energy). The resulting MS3 spectra were monitored at m/z 100–500 in the Orbitrap, which operated at a resolution of 60,000, AGC target of 1e5, and maximum injection time of 120 ms. The same parameters were used in the remaining three scan events, and the isolation windows for MS3 in scan event two, three, and four were 0.8, 1, and 1.3 Da, respectively.

MS data processing

The raw files were processed using Proteome Discoverer (PD, version 2.1.1.21). SEQUEST^{HT} was employed to search against a protein database for the genus *Nicotiana*, which was downloaded from the National Center for Biotechnology Information (NCBI, https://www.ncbi.nlm.nih.gov) and cleaned by removing incomplete sequences with length less than 50 amino acid residues. The search algorithm in the processing workflow used 10 ppm and 0.6 Da as mass tolerance for MS1 and MS2, respectively. A maximum of two missed cleavage sites was selected for the trypsin digestion. Carbamidomethyl of cysteine (+ 57.021 Da) was set as static modification, and oxidation of methionine (+ 15.995 Da) as well as phosphorylation of serine, threonine and tyrosine (+ 79.966 Da) were specified as dynamic modifications. Adding of TMT 6-plex tags (+ 229.163 Da) on both lysine residues and peptide N-terminus was set as dynamic modifications. Peptide spectra matches (PSMs) were validated by Percolator, and the results were filtered using 1% false discovery rate (FDR) as a cutoff. Localization of phosphorylation sites was performed with the PD ptmRS node. The data were further filtered using the consensus workflow with the following parameters: two as the minimum number of peptides for protein identification, 1% as the confidence threshold for protein FDR validation, 50 as the co-isolation threshold for reporter ion quantification, and 10 as the reporter ion S/N threshold.

Both the raw and searched data have been deposited to the ProteomeXchange Consortium via the PRIDE partner repository with the project accession of PXD012442 (Username reviewer93744@ebi.ac.uk, Password bZkhBVB2).

Statistics and bioinformatics

For global analysis, the raw protein abundance values exported from PD were log2 transformed, and the median values of each quantification channel were aligned for normalization. Proteins quantified in all six TMT channels were retained for further analysis. The Student *t* test was used for statistical significance analysis. To correct for multiple-test error, the obtained p values were adjusted by the Benjamini–Hochberg method with a FDR < 0.01. A further fold change of at least 1.5 was used to define significantly changed proteins. For phophoproteome analysis, the normalization factors obtained in the global settings were applied to correct possible variations in total protein loading. The same statistical test and criteria in defining significance for global proteome analysis were applied in the phosphoproteomics analysis.

Principal component analysis (PCA) was performed using the prcomp function in the R 'base' package. The first two PCs were plotted. For gene ontology (GO) analysis, statistically significant proteins were blasted against the well-annotated *Arabidopsis* database (https://www.arabidopsis.org/) using local BLAST (v2.8.1, downloaded from the NCBI). The top hits were considered as the homologous proteins in *Arabidopsis*, and were used for enrichment analysis with agriGO (Tian et al. 2017). Fisher exact test was chosen as the statistical test method, and Hochberg (FDR) was used for multi-test adjustment.

Western blotting of MPK4 expression and potential substrates

For *Bn*MPK4 expression, protein samples were separated by 12% SDS-PAGE, transferred to nitrocellulose membrane and incubated with a purified anti-FLAG antibody (Sigma-Aldrich, St. Louis, MO, USA) at a dilution of 1:3000. Anti-mouse IgG conjugated to horseradish peroxidase (Pierce, Rockford, IL USA) was used as secondary antibody at a dilution of 1:10,000. Protein signals were detected using ECL substrates (Thermo Scientific, Rockford, IL, USA). Ponceau S stained RuBisCO band or Coomassie stained protein band was used as an equal loading control. For detecting potential *Bn*MPK4 substrates (6-histidine-tagged TCP8 and TAP46), the procedure was the same as above except that a monoclonal anti-histidine antibody (Sigma-Aldrich, St. Louis, MO, USA) at a dilution of 1:5000, and an anti-mouse IgG conjugated to horseradish peroxidase (Pierce, Rockford, IL, USA) at a dilution of 1:10,000 were used.

Validation of putative *Bn*MPK4 substrates

Genes of interest were cloned to intermediate vectors pSC (Stratagene), and then sub-cloned into pET28a vector for recombinant protein expression. Primers used for cloning were 5′-CGCCATATGG CGATGGAACT CTCTGATTTA CAAAATAAC-3′ and 5′-ATTTGCGGCC GCTTTATGTT TGGATCATCA TCTTCGCTATC-3′ for a TF TCP8, and 5′-CGCCATATGG CGATGGGCGA ACTGAACATG CAA GAGATG-3′ and 5′-ATTTGCGGCC GCTTTAACCA CAA GGAGTTA GCTTCTTGTTACC-3′ for a PP2A regulatory

subunit TAP46, respectively. RNA extraction, cDNA synthesis, polymerase chain reaction (PCR) amplification, ligation, bacteria transformation, and heterozygous expression in the *Escherichia coli* strain BL21 (DE3) cells were performed as described previously (Zhang et al. 2015). The recombinant proteins were purified using a PrepEase™ histidine-tagged protein purification kit (Affymetrix, Inc.) following the manufacturer's instructions. For in-solution kinase assay, 2 µg of putative substrate proteins were incubated with 1 µg of MPK4 in the kinase reaction buffer (25 mM Tris–HCl, pH 7.5, 10 mM $MnCl_2$, 10 µM ATP, and 5 µCi γ-^{32}P ATP) at 30 °C for 30 min. The reaction was stopped by adding equal volume of SDS-PAGE sampling buffer (50 mM Tris–HCl, pH 6.8, 2% SDS, 10% glycerol, 12.5 mM EDTA, 0.02% bromophenol blue and 1% β-mercaptoethanol). The reaction mixture was separated on a SDS-PAGE gel, and the phosphorylation on substrate was determined by autoradiography as previously described (Zhang et al. 2015).

Results

Transient activation of MPK4 in *N. benthamiana*

To determine the downstream signaling pathways of a *B. napus* MPK4 (*Bn*MPK4), we generated constructs that allowed for the expression of *Bn*MPK4^{CA} and *Bn*MPK4^{IN} *in planta* (Zhang et al. 2015). Both mutants, along with *Bn*MPK4^{WT} and the vector control (VC) were expressed in *N. benthamiana* leaves (Fig. 1a). The protein abundance of the MPK4s was determined by Western blot. While both *Bn*MPK4^{WT} and *Bn*MPK4^{IN} can be readily detected from 1 to 4 days post infiltration (dpi), the expression of *Bn*MPK4^{CA} decreased significantly at 3 dpi and was completely absent at 4 dpi (Fig. 1b). We previously showed that *N. benthamiana* leaves infiltrated with the *Bn*MPK4^{CA} construct accumulated high level of reactive oxygen species (ROS) and displayed hypersensitive response (HR)-mimic cell death. In contrast, plants expressing *Bn*MPK4^{WT} and *Bn*MPK4^{IN} showed no visible differences from plant infiltrated with VC (Zhang et al. 2015). Thus, protein degradation associated with the cell death process may result in the disappearance of *Bn*MPK4^{CA}. Since the expression of *Bn*MPK4^{CA} peaked at 2 dpi,

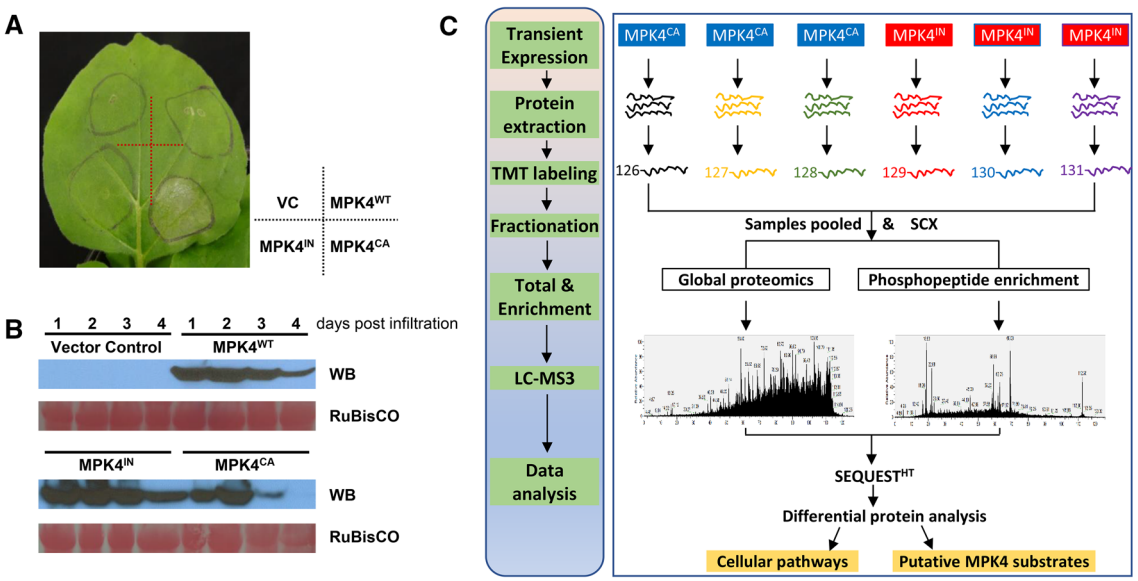

Fig. 1 Experimental setup of MPK4 genetic engineering and mass spectrometry to determine MPK4-triggered changes in proteome and phosphoproteome. **a** Phenotype of *N. benthamiana* leaves transiently expressing MPK4 variants. *VC* vector control, *MPK4^{WT}* wild type MPK4, *MPK4^{IN}* inactive MPK4, *MPK4^{CA}* constitutive active MPK4. **b** Time course of MPK4 expression. Protein samples were extracted from *N. benthamiana* leaves expressing different MPK4 variants, and the expression level was determined by Western blot (WB) using an anti-FLAG antibody. Ponceau S staining of RuBisCO was used as a loading control. **c** Workflow of quantitative proteomics. Ten infiltrated leaf sections expressing either MPK4^{CA} or MPK4^{IN} were pooled together as one biological replicate. Each MPK4^{CA} or MPK4^{IN} had three biological replicates. Proteins were extracted and then digested with trypsin. The resulting peptides from each sample were labeled with TMT 6-plex. Following labeling, all the samples were pooled and the combined sample was fractionated on SCX chromatography into six fractions, and 5% of each fraction was used for total protein analysis. The remaining 95% of each fraction was enriched for phosphopeptides. Tandem mass spectrometry data were acquired on an Orbitrap Fusion Lumos Tribrid MS. The raw spectra were processed using Proteome Discoverer with SEQUEST^{HT}, and statistical analysis was implemented with R

leaf tissues at 2 dpi were collected to assess the contribution of MPK4 activity in cell signaling. The kinase activities of three versions of MPK4s were determined by in-gel kinase assay, with a strong phosphorylation on MKS1 (MPK4 substrate 1) detected only by *Bn*MPK4^{CA} (Fig. S1). *Bn*MPK4^{WT}, similar to *Bn*MPK4^{IN}, did not show strong kinase activity, in line with the observation that *in planta* expressed MPK4 are not activated at basal conditions (Zhang et al. 2019). In order to minimize potential variation among different leaves, *Bn*MPK4^{CA} and *Bn*MPK4^{IN} were expressed symmetrically in the same leaf for the following experiments. The biological replicates were from different plants.

Quantitative proteomics for studying MPK4 signaling

Taking advantage of genetic engineering of MPK4 activity, we next developed a MS-based method that allowed us to quantitatively compare the proteomes and phosphoproteomes of *N. benthamiana* leaves expressing *Bn*MPK4^{CA} and *Bn*MPK4^{IN} (Fig. 1c). The global proteomics workflow consisted of protein extraction, trypsin digestion, isobaric stable isotope labeling for quantification, and ultra-high performance LC–MS. For phosphoproteomics, we used a TiO_2 and ZrO_2 method for phosphopeptide enrichment. For quantitative analysis, we employed TMT 6-plex reagents to label six biological samples (n = 3 for each group). Thus, the effect of MPK4 activation on both the proteome and phosphoproteome can be compared simultaneously.

Confident identification and accurate quantification of proteins are necessary for a successful proteomics experiment. To demonstrate that this workflow produces high quality data, we evaluated several key parameters in data acquisition. The six fractions of the non-enriched samples resulted in the identification of 29,202 high confident (FDR < 1%) PSMs. The distribution of Δm/z (the difference between the theoretical and the experimental m/z) was within 0.01 Da (Fig. S2a), demonstrating accurate measurement of precursor ions in the high-field Orbitrap. The goodness of fit between the acquired MS/MS spectra and the theoretical b and y ions (generated in silico from the database searching) was measured by the cross-correlation score (XCorr; Eng et al. 1994). As shown in Fig. S2b, the median values of XCorr for majority of the PSMs, bearing + 2 and + 3 charges, were over 3. To quantify the peptides, we employed a MultiNotch MS3 method in which multiple MS2 fragment ions were co-isolated and fragmented to generate TMT reporter ions (McAlister et al. 2014). Analysis of the intensity of the reporter ions revealed that 89.2% of the PSMs displayed a ratio of signal to noise (S/N) over 30 (Fig. S2c), confirming that the MultiNotch MS3 method produces high quantification signals of the isobaric tags. In addition, the specificity of the PSMs was evaluated by ΔCn (the lower, the better), which scores the difference between the highest-scoring PSM and the currently selected PSM that can be identified by the same MS/MS spectra. Figure S2d showed that 98.2% of the high confident PSMs had a ΔCn value of 0, ensuring that only the top ranking PSMs were chosen for further analysis. The quantification reproducibility among biological replicates was assessed by Pearson correlation, which showed an average of correlation efficiency of 0.98 (Fig. S2).

Activation of MPK4 resulted in drastic changes in both the proteome and phosphoproteome

To relate MPK4 activation and proteomic changes in *N. benthamiana*, we performed a PCA. This unsupervised data-driven approach allows for data complexity reduction as linear combinations of multivariate protein abundances are presented as the PCs. As shown in Fig. 2a, *Bn*MPK4^{CA} and *Bn*MPK4^{IN} samples at the total protein level can be clearly separated by PC1, which can explain 81.6% of the total variance. In addition, PC2 captured another 9.5% of overall variance within the dataset. The next two orthogonal components accounted for 4.6% and 2.6% of the variance, respectively; making the first four components explained over 98% of the total variance cumulatively. In addition, the distance within the three *Bn*MPK4^{CA} biological replicates was larger than that of *Bn*MPK4^{IN} samples, indicating more biological variability introduction by the MPK4 activation. Nonetheless, the distance within the biological replicates was much smaller than that between the *Bn*MPK4^{WT} and *Bn*MPK4^{CA} groups, demonstrating the robustness of the segregation. Similar PC loading patterns were observed in the phosphopeptide dataset (Fig. 2b). Thus, PC1 for both cases served coarsely as the "MPK4 activity" axis, suggesting that alteration in MPK4 activity resulted in profound changes at both the overall proteome and the phosphoproteome in *N. benthamiana* leaves.

Next, we evaluated the overall changes in protein abundance, expressed as log2 transformed ratio between the *Bn*MPK4^{CA} and *Bn*MPK4^{IN} (log2 fold change) (Fig. 2c, d; Table S1). While MPK4 activation introduced perturbation on the global proteome at both directions of increase and decrease symmetrically (Fig. 2c), the change at the phosphoproteome level was predominantly shifted toward the increased direction (Fig. 2d; Table S3). Furthermore, in contrast to similar amplitude of decrease in both the proteome and phosphoproteome, we observed much higher amplitude of increase in the phosphoproteome. Overall, these data provided strong validation of the responsiveness of the biological system to *Bn*MPK4^{CA} and the sensitivity of our technology.

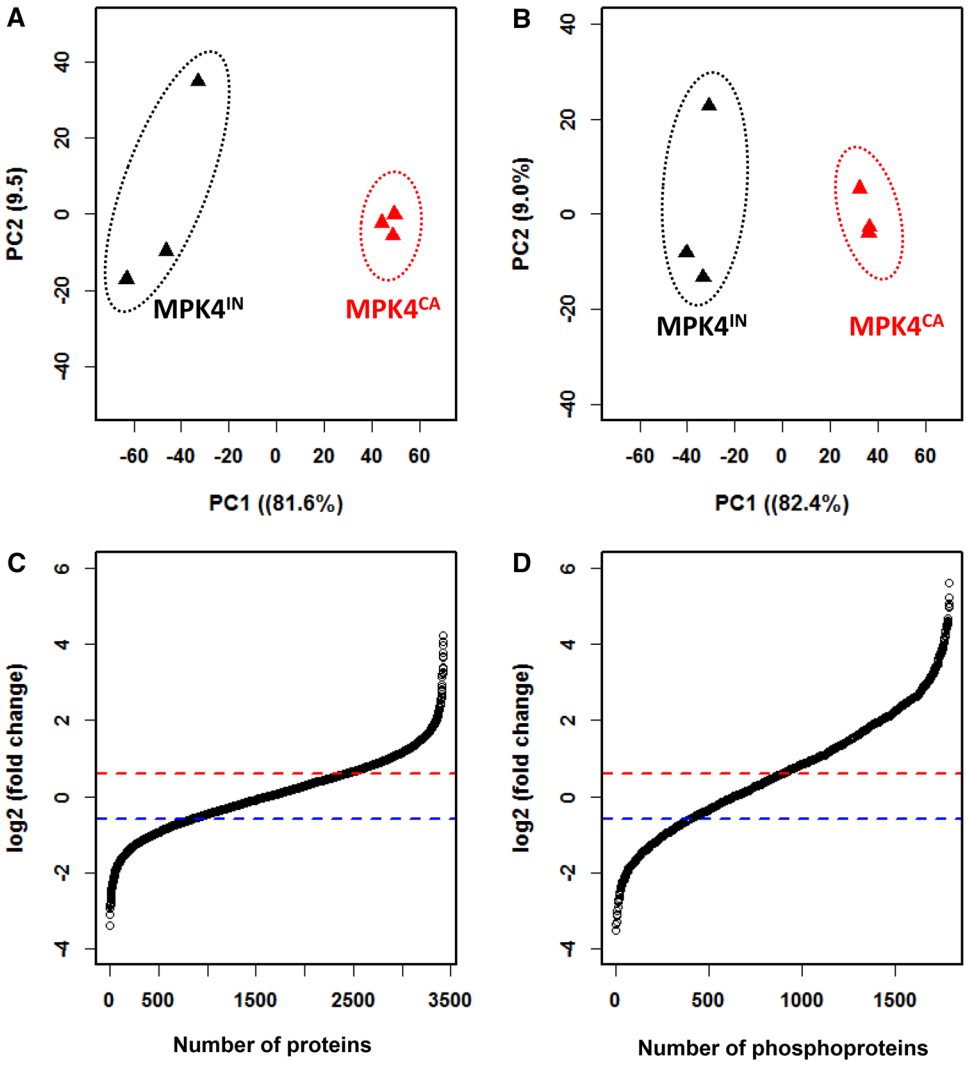

Fig. 2 MPK4 activation affects both the proteome and phosphoproteome. **a** PCA of the global proteome data separates MPK4^{CA} and MPK4^{IN}-expressing leaves. **b** PCA analysis of the phosphoproteome of MPK4^{CA} and MPK4^{IN}-expressing leaves. **c** Overview of the proteome change. Proteins were ranked based on the fold change (MPK4^{CA} over MPK4^{IN}), and the log2 fold change was plotted on y axis. Dotted blue and red lines indicate log2 fold change of − 0.58 and 0.58, corresponding to 1.5-fold decrease, or increase in abundance, respectively. Even distribution of the overall change was noted. **d** Overall pattern of phosphoproteome changes. MPK4 activation caused a shift toward increase in protein phosphorylation

Functional analysis of differentially regulated proteins

To visualize the global proteomics data, we created a volcano plot with the extent of change (in log2 fold change between *Bn*MPK4^{CA} and *Bn*MPK4^{IN}) on the x axis and the statistical confidence (adjusted p value, or q value) on the y axis. As seen in Fig. 3a, majority of the proteins fall below the 0.01 q value cutoff. Further applying a fold change of 1.5 as a cutoff showed 177 and 145 proteins significantly decreased and increased, respectively (Fig. 3b; Table S3).

To decipher key cellular pathways that are modulated by the MPK4 activation, we focused on the 322 significantly changed proteins for GO enrichment. Activation of MPK4 induces ROS production and HR-mimic cell death (Zhang et al. 2015). Accordingly, GO analysis revealed significant enrichment in biological processes such as oxidation reduction, plant-type HR and cell death. In line with the notion that MPK4 is activated by stress, GO terms such as response to stress, protein turnover (ubiquitin-dependent protein catabolic process), and defense response have also been enriched (Fig. 3c). Clustering analysis of significantly changed proteins related to stress response showed that there were more increased proteins than decreased proteins caused by MPK4 activation (Fig. S4). Unbiased bioinformatics analysis also showed some previously unknown cellular mechanisms by which MPK4 exerts its function. For example, the enrichment of oxylipin biosynthetic process (mostly decreased, as shown in Fig. S5), jasmonic acid metabolic process, and fatty acid metabolic process suggests MPK4 modulates these processes in a kinase-activity dependent manner.

To further understand MPK4-induced pathways, we further performed enrichment analysis with the significantly decreased and increased proteins separately (Fig. S6). We found that the decreased proteins are predominately enriched in metabolic processes such as carbohydrate and amino acid metabolism, while the increased proteins are enriched in

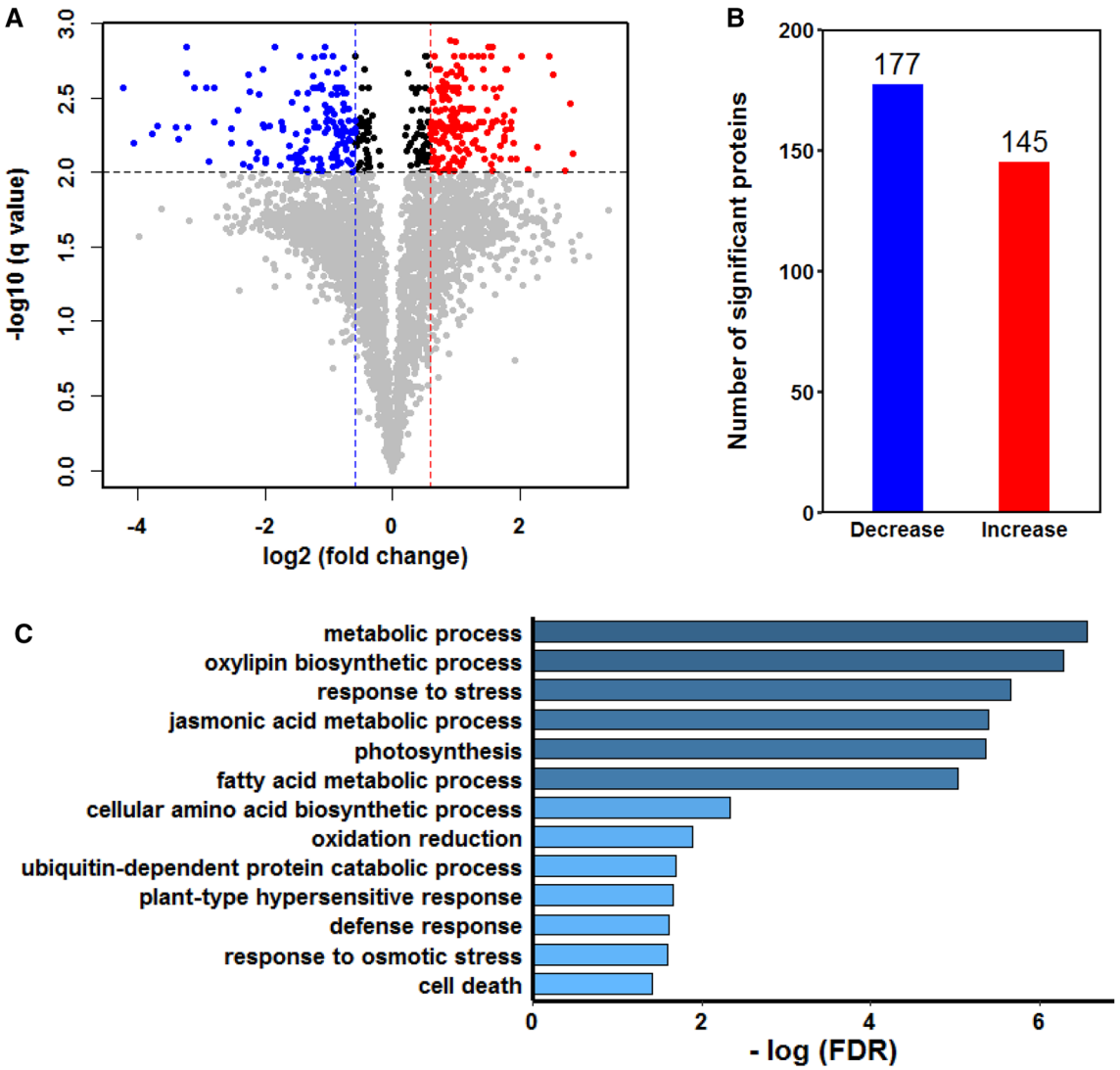

Fig. 3 Global proteome response to MPK4 activation. **a** Volcano plot showing difference in global proteomes between MPK4^{CA} and MPK4^{IN}-expressing leaves. The log2 fold change (MPK4^{CA}/MPK4^{IN}) was plotted on the x axis, and − log10 p value (Benjamini–Hochberg corrected, thus q value) was plotted on the y axis. Dashed lines indicate significance cutoff (vertical for q value of 0.01, or − log10 q value of 2; vertical for fold change of 1.5, or log2 fold change of 0.58). Significantly increased or decreased proteins are color-coded in red and blue, respectively. **b** Number of significantly increased-(in red) and decreased-(in blue) proteins. **c** Enriched biological processes of significantly changed proteins. The top GO items were ranked by the enrichment score and − log FDR (adjusted p value)

stress response. This observation is in line with the view that overexpression of *Bn*MPK^{CA} activates plant defense.

Functional analysis of differentially regulated phosphoproteins

Analysis of the phosphopeptide-enriched samples yielded > 2000 non-redundant phosphorylation sites on 1791 phosphopeptides that can be mapped to 1113 phosphoproteins (Table S3). While a significant portion of the phosphoproteins (755 out of 1113) were identified by one unique phosphopeptide, the remaining 32% phosphoproteins (358 out of 1113) were identified by at least two unique phosphopeptides (Fig. S7a). Since phosphorylation events are site-specific, we wonder whether the changes in phosphorylation levels of distinct phosphopeptides within the same protein correlates with each other. Using 208 phosphoproteins with 2 phosphopeptides in our dataset (Fig. S7a), we found an overall poor correlation (correlation efficiency as 0.57, Fig. S7c). Therefore, data analysis for phosphoproteomics was performed at the peptide level. Using FDR of 0.01 and fold change of 1.5 as cutoffs for defining significance, we found that 195 and 402 phosphopeptides were decreased and increased in phosphorylation, respectively, following the

MPK4 activation (Fig. 4a, b; Table S4). These peptides corresponded to 472 phosphoproteins, with the majority identified by 1 unique phosphopeptide (Fig. S7b). For 67 significantly changed phosphoproteins with 2 phosphopeptides, the correlation was much higher than that for all the detected proteins with 2 phosphopeptides (Fig. S7d), suggesting that significant changes of multiple phosphorylation events on the same protein tend to occur at the same directionality.

Next, we wondered whether the changes at the protein phosphorylation levels are due to a similar increase at the protein expression levels. To this end, we compared the abundance change, expressed as log2 fold change of *Bn*MPK^{CA} over *Bn*MPK^{IN}, between the global proteome and the phosphoproteome for 212 phosphopeptides whose proteins have also been quantified in the global analysis. As shown in Fig. S8, only 4% (9 out of 212) showed significant increases at both levels (red dots). Pearson correlation analysis showed a correlation coefficient of only 0.32, indicating that the enhanced phosphorylation may not be attributed to increase in global protein expression.

In agreement with the global proteomics results (Fig. 3c), GO enrichment of significantly changed phosphoproteins also revealed that MPK4 activation is involved in the regulation of stress response (abiotic stimulus), protein turnover

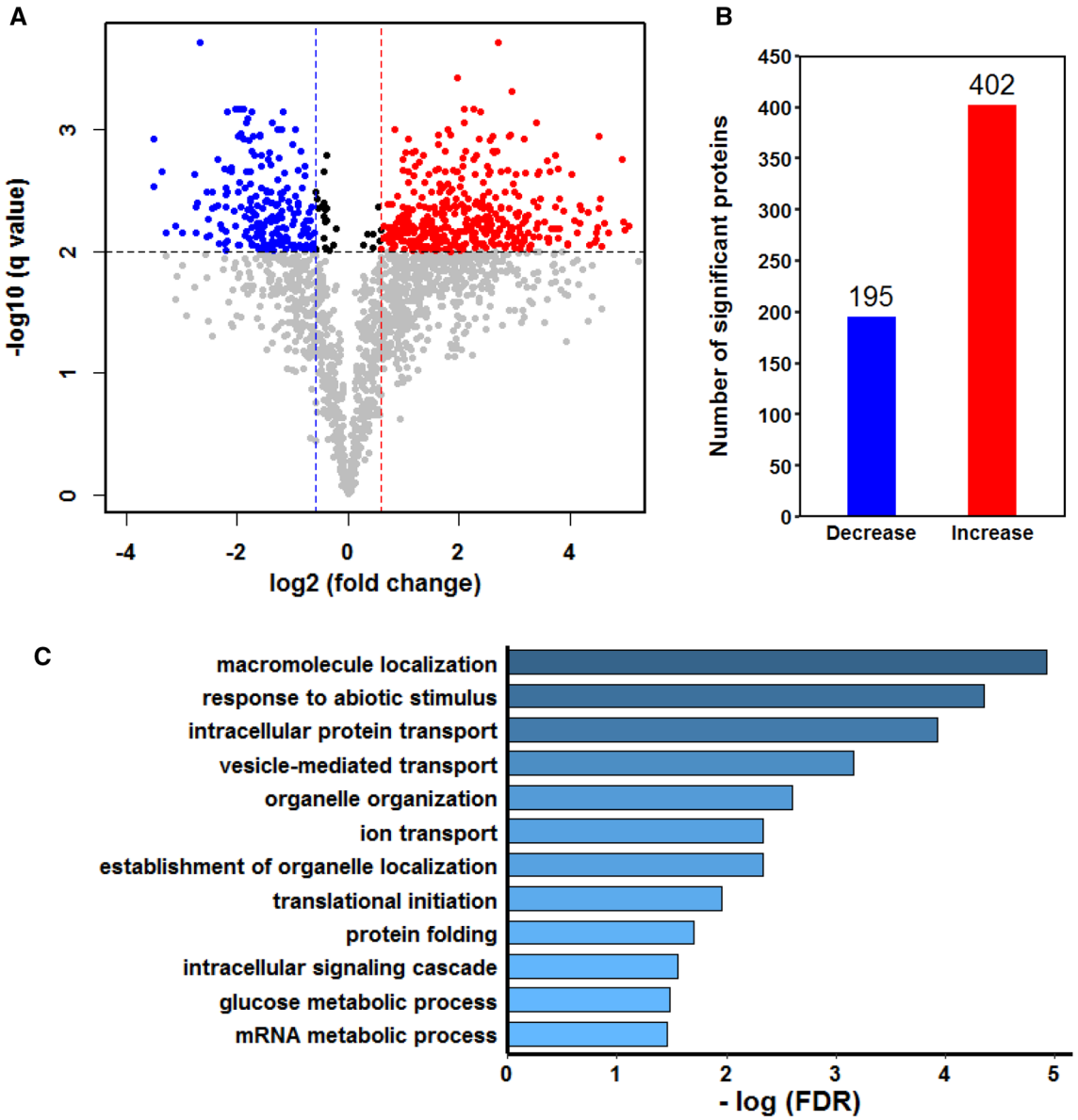

Fig. 4 Phosphoproteome response to MPK4 activation. **a** Volcano plot showing difference in phosphoproteomes between MPK4^{CA} and MPK4^{IN}-expressing leaves. The same criteria in in Fig. 3a were used to define differential phosphoproteins. **b** Number of significantly increased and decreased phosphoproteins. **c** Enriched biological processes of significantly changed phosphoproteins

(translational initiation), and metabolic processes (glucose and mRNA metabolism), as shown in Fig. 4c. Notably, proteins with MPK4-dependent phosphorylation were also enriched in intracellular signaling cascade, ion transport and protein transport and other macromolecule localization (Fig. 4c). Thus, our phosphoproteomic analysis was robust in identifying proteins and pathways previously not linked to MPK4 functions. Similar to global proteome analysis, we also performed the enrichment analysis with decreased and increased phosphoproteins separately (Fig. S9). More GO items were enriched from the increased phosphoproteins, with higher level of statistical significance, than from the decreased proteins. More importantly, pathways closely related to MPK4 functions such as protein folding and responses to stress are only enriched in the increased phosphoproteins.

Identification and validation of MPK4 substrates

The rich information from phosphoproteomics provides an opportunity to identify potential MPK4 substrates. We used the increased phosphopeptides in *Bn*MPK4^{CA} samples as our initial candidate list, and further filtered the list based on the subcellular localization of the corresponding proteins. This is because MPK4 is localized in the nucleus and cytoplasm (Petersen et al. 2000; Berriri et al. 2012). This resulted in 76 phosphopeptides, mapped to 71 proteins, as putative MPK4 substrates (Table S5). Figure 5a showed that these phosphopeptides clustered into two major groups, with one group showing > 8-fold increase of phosphorylation in *Bn*MPK4^{CA} compared to *Bn*MPK^{IN}. Remarkably, motif analysis showed that phosphorylation on the putative substrate peptides were predominantly on serine (S) and threonine (T) residues (Fig. 5b), consistent with the fact that MPK4 is an S/T-specific kinase. In addition, proline (P) was significantly overrepresented following the S/T phosphorylation sites, further supporting that they are likely to be genuine MPK4 substrates.

To validate our proteomics findings, we performed kinase assays to determine whether MPK4 can phosphorylate the putative targets in vitro. As shown in Fig. 5, neither TCP8 nor TAP46 showed autophosphorylation by itself. However, upon incubation with *Bn*MPK4, strong phosphorylation can be detected on these proteins, demonstrating that *Bn*MPK4 can effectively phosphorylate both TCP8 and TAP46. Since these two proteins have not been linked to the kinase, our data suggest that they may be new MPK4 substrates.

Discussion

Transient expression of *Bn*MPK4^{CA} in *N. benthamiana* leaves allowed the kinase to phosphorylate its substrate proteins *in planta*. Non-substrate proteins should exhibit similar levels of phosphorylation in both the *Bn*MPK4^{CA} and *Bn*MPK4^{IN} samples. Thus, activation of MPK4 is expected

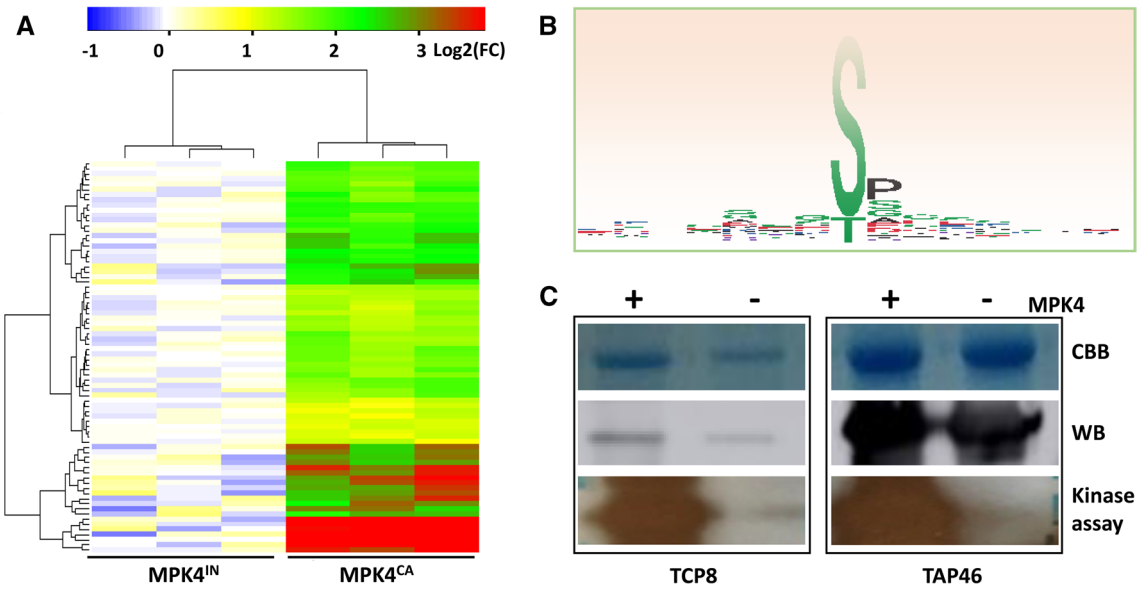

Fig. 5 Screening and validation of putative MPK4 substrates. **a** Heatmap showing phosphorylation patterns of putative MPK4 substrates. **b** Motif analysis of putative substrate peptides. **c** Validation of TCP8 (63 kDa) and TAP46 (51 kDa) as newly identified MPK4 substrates by kinase assay. Top panel, Coomassie blue staining of TCP8 (left) and TAP46 (right). Middle panel, Western blot using anti-His tag antibody to detect TCP8 (left) and TAP46 (right). Bottom: phosphorylated TCP8 by MPK4 (+) and phosphorylated TAP46 by MPK4 (+). TCP8: transcription factor TCP8-like (Accession No. XP_016514875.1); TAP46: PP2A regulatory subunit TAP46-like (Accession No. XP_016507074.1)

to result in elevated phosphorylation of bona fide substrates. As a control, the proteome and phosphoproteome of plants expressing *Bn*MPK4^{IN} were used to evaluate possible perturbations introduced by ectopic expression of the MPK4 protein. Thus, quantitative comparison of the phosphorylation levels between the *Bn*MPK4^{CA} and *Bn*MPK4^{IN} samples can identify MPK4-induced phosphorylation events in an unbiased manner. We chose to use *Bn*MPK4^{IN}, instead of wild type MPK4 (*Bn*MPK4^{WT}), as a control so that we have a clean background and thereby add confidence to the *Bn*MPK4^{CA} mediated phosphorylation. It should also be noted that kinase-substrate interactions are highly dynamic and context-dependent. Thus, the method developed here may be modified to identify tissue/cell-specific or developmental stage-specific kinase substrates. On the other hand, using an easy-to-implement heterozygous expression system would allow for the identification of conserved protein kinase substrates. Additionally, the well-characterized *Bn*MPK4 in our lab was used as a MPK4 representative in this study, given the high sequence similarity of MPK4s across different plant species (Zhang et al. 2014) and the highly conserved nature of MPK signaling in general (Hamel et al. 2006).

Our understanding of how MPK4 functions in plants has increased substantially, largely from genetic manipulation and analysis of mutants with altered phenotypes. For example, we and others have previously demonstrated that overexpression of *MPK4* leads to changes in many aspects of plant physiology including ROS production, growth and development, cell death and resistance to pathogen infection (Wang et al. 2009; Berriri et al. 2012; Zhang et al. 2015; Liu et al. 2018). The essential roles of MPK4 in these processes had been confirmed in other studies where *MPK4* was silenced (Hettenhausen et al. 2012; Liu et al. 2011; Petersen et al. 2000). With these findings has come the realization that MPK4 is a multifaceted kinase playing central roles in a diverse range of biological processes. Thus, a systematic approach is required to appreciate the complicated signaling pathways downstream of MPK4. Using an unbiased proteomics workflow in conjunction with genetic engineering of kinase activity, we found that MPK4 activation results in drastic changes of the global proteome. As expected, MPK4 activation also perturbs the phosphoproteome, from which we have identified potential MPK4 substrate proteins. These findings demonstrated that proteomics represents a robust tool in tackling two of the most important questions in kinase signaling: what are the downstream cellular activities and what are the substrates through which the signal is relayed.

One of the most striking differences between the *Bn*MPK4^{CA} and *Bn*MPK^{IN} infiltrated leaves is that the former displayed increased ROS production (Zhang et al. 2015). In line with this, our proteomics data showed that respiratory burst oxidase homolog (RBOH) had a 16-fold increase in protein abundance (Table S2). A previous study has shown that MPK signaling regulates oxidative burst (Asai et al. 2008), and the increase of RBOH at the protein level suggests that MPK4 induces the accumulation of RBOH. This is in contrast to a calcium-dependent protein kinase 5, which directly phosphorylates RBOH to promote oxidative burst for plant defense (Dubiella et al. 2013). Remarkably, MPK4 activation also resulted in increase of peroxidases 1 and 2 (Table S2), key members of antioxidant defense system to detoxify ROS. This implies that MPK4 activates both the ROS producing and ROS quenching systems. The high levels of ROS production and the activation of the quenching systems are indicative of the specific signaling role of ROS. Quickly returning to ROS homeostasis after the signaling role has been fulfilled may be required to prevent cellular oxidative damage (Pitzschke et al. 2009b).

Besides redox regulation, other significantly increased proteins include pathogenesis-related (PR) protein and Nb cell death marker. PR proteins are molecular markers for plant pathogen response. The role of MPKs in *PR* gene expression has been determined using quantitative reverse transcription-PCR analysis. The data showed an up to 7-fold increase at the mRNA level of *PR1* in MKK3 overexpressing lines of *Arabidopsis* (Dóczi et al. 2007). Recently, similar gene expression analysis showed that *PR1* is elevated in an *mkk1/2* mutant, which exhibits constitutive defense response (Lian et al. 2018). Our proteomics data demonstrated increases of PR proteins following the MPK4 activation, in line with the idea that MPKs regulates PR protein levels in plant defense. In response to pathogen, MPK could also lead to HR-mimic cell death (Ren et al. 2006; Zhang et al. 2015). However, the molecular pathways involved are not clear. Our proteomics data revealed a 7-fold increase in Nb cell death marker (Accession No. CBK52316). Other significantly changed proteins in the cell death process include patatin-like protein 3 (Accession No. XP_016482549.1), 8-hydroxygeraniol dehydrogenase-like (Accession No. XP_009783463.1), catalase isozyme 1 (Accession No. XP_009792372.1), and class IV chitinase (Accession No. BAF44533.1), indicating that lipid degradation, redox control and cell wall modification are involved in the MPK4-induced cell death.

Global proteomics also revealed that many metabolic processes including photosynthesis and fatty acid metabolism were affected by MPK4 activation. Emerging evidence suggests that MPKs could serve as converging points of multiple upstream signals to orchestrate many distinct processes. Such a role for MPK3/6 has been recently described in balancing the trade-off between plant growth and defense (Su et al. 2018). We showed in this study that MPK4 activation attenuates key enzymes in fatty acid biosynthesis such as 3-hydroxyacyl-[acyl-carrier-protein] dehydratase FabZ (Accession No. XP_016512868.1). Consistent with

the down-regulation of photosynthetic genes in other studies (Hettenhausen et al. 2012; Su et al. 2018), we also observed that many proteins in photosynthesis were decreased including Photosystem II protein D1 (Accession No. CAA25252.1) and chloroplastic magnesium-chelatase subunit ChlH (Accession No. XP_016469478.1). It is plausible that MPK4 plays a role in plant adjustment of its priority for defense or growth during its life cycle.

Based on our phosphoproteomics data and functional screening, we identified 71 proteins as potential MPK4 substrates. Some of these proteins have been shown to interact with MPK4 in other plant species. For example, WRKY33 functions downstream of MPK4 in camalexin production in *Arabidopsis* (Qiu et al. 2008). In our study, we found significant phosphorylation on a double WRKY type TF (Accession No. BAI63295.1), homolog of WRKY33 in *N. benthamiana*. This not only validates our method for mining MPK4 substrates, but also supports the evolutionary conservation of substrate specificity across different plant species (Doczi et al. 2012). Furthermore, Cui et al. showed that heat shock protein 90 (HSP90) facilitated the interaction between MPK4 and a bacterial effector avirulence protein Avr B (Cui et al. 2010). In line with this finding, we found that HSP70-HSP90 organizing protein 2 (Accession No. XP_009595716.1) is significantly phosphorylated upon MPK4 activation, suggesting that MPK4 may direct the association of HSP90 with other proteins under stress.

Physical interaction is required for phosphorylation to occur between a MPK and its substrates. Previously, we carried out an immunoprecipitation coupled with proteomic analysis to identify MPK4-interacting proteins. Significantly, we found six proteins present in both the list of putative MPK4 substrates (this study) and the list of MPK4-interacting proteins (Zhang et al. 2019). They are enhancer of mRNA-decapping protein 4-like (AT3G13300), FAM188A-like (AT1G43690), poly-A binding protein (AT1G49760), auxin-induced protein PCNT115-like (AT1G60710), stem-specific protein TSJT1-like (AT4G27450), and pantothenate kinase 2 isoform X1 (AT4G32180). In addition, we found that two proteins in our list, protein-lysine *N*-methyltransferase Mettl10-like (AT1G66680) and stem-specific protein TSJT1-like (AT4G27450), which were also identified as MPK4 substrates in a recent study (Rayapuram et al. 2018). Identification of these proteins in two independent experiments with orthogonal techniques provides strong confidence of our findings.

We also compared our list of putative MPK4 substrates to lists of potential MPK3/6 substrates published by other groups (Hoehenwarter et al. 2013; Lassowskat et al. 2014). In both published studies, a constitutively active version of MPK3/6 kinase (*Nicotiana tabacum* MEK2^{DD} and *Petroselinum crispum* MKK5^{DD}) was transiently activated and the resulting phosphoproteomes were compared to the controls. Both reported more than 140 kinase substrates, among which 6 (AT1G43690, AT4G11740, AT5G13020, AT3G13300, AT5G51300, AT2G43680) and 4 proteins (AT2G38470, AT1G62300, AT3G13300, AT5G51300) were overlapped with our list, respectively. It is interesting that two proteins, AT3G13300 (Transducin/WD40 repeat-like superfamily protein) and AT5G51300 (splicing factor-related), were identified as MAP kinase substrates in all the three studies, supporting the notion that a single protein substrate can be phosphorylated by multiple kinases.

Importantly, majority of the potential substrates in our list are newly identified that fall into several categories (Table S5). The first group consisted of TFs including TCP8-like (Accession No. XP_016514875.1), probable TF PosF21 (Accession No. XP_016434211.1), and bHLH130-like (Accession No. XP_016485356.1). The exact physiological functions of these TFs are not known. Other potential substrates belong to signaling proteins themselves, including serine/threonine-PK SRK2A (Accession No. NP_001312448.1), developmentally-regulated G-protein 2 (Accession No. XP_016459224.1), SNF1-related PK regulatory subunit beta3 (Accession No. XP_009629026.1), calmodulin-binding receptor-like cytoplasmic kinase 2 (Accession No. XP_016457899.1), and PP2A regulatory subunit TAP46-like (Accession No. XP_016507074.1). The identification of other PKs and phosphatases as substrate of MPK4 defies the conventional belief that MPK4 is the terminal kinase of a linear MPK cascade. Rather, it supports the emerging notion that MPKs can interact with other kinase-based signaling pathways, as have already been demonstrated in the case of MPK4 and MEEK2 in *Arabidopsis* (Kong et al. 2012). The last group of potential MPK4 substrates contains proteins of diverse functions in RNA binding, nuclear transport, stress response, and protein degradation, suggesting these proteins could be the molecular partners with which MPK4 operates in a diverse array of cellular processes.

We anticipate that the approach described here will be useful across a range of applications to identify kinase substrates and profile downstream signaling events. The efficacy of this approach for substrate screening is contingent upon the relevance of experimental setup and quality of proteomic analysis. Although it has been shown that MPK4^{CA} maintains its substrate specificity, the test was performed with only few known proteins (Berriri et al. 2012). Whether MPK4^{CA} or other constitutive active kinases would maintain their specificity when tested with a broad range of substrates is unknown. This issue could be addressed by using physiologically relevant stimulations to activate the kinase of interest. In addition, *N. benthamiana* was used to transiently express *Bn*MPK4 in this study, for which *Bn*MPK4 may not function identically to *Nb*MPK4. Nevertheless, such a system was chosen to test the feasibility of this approach and to

identify common substrates across different species. Finally, a key aspect of this work is its use of unbiased large-scale proteomics and phosphoproteomics, a field with tremendous improvement in both coverage and quantification recently (e.g., the timsTOF). Future work can definitely benefit from these technological advancements to improve understanding of MPK signaling cascade.

Acknowledgements The authors thank Dr. Xiaoen Huang for providing *N. benthamiana* seeds, Dr. Alice Harmon for helpful discussions, and Dr. Joshua A. Silveira for mass spectrometry data acquisition. This research was supported by Grants from the National Science Foundation (MCB 0818051 and MCB 1412547 to S. Chen).

Author contributions T.Z., W.S., and S. Chen developed the experimental plan, and T.Z. performed most of the experiments and data analysis. S. Chhajed conducted protein expression and in-solution kinase assay. J.D.S. performed infiltration and sample collection. G.F. built the *Nicotiana* database and assisted with bioinformatics analysis. T.Z. drafted the manuscript and S. Chen finalized the paper. All authors reviewed and approved the manuscript.

Compliance with ethical standards

Conflict of interest The authors declare no competing financial interest.

References

Andreasson E, Jenkins T, Brodersen P, Thorgrimsen S, Petersen NHT, Zhu SJ, Qiu JL, Micheelsen P, Rocher A, Petersen M, Newman MA, Nielsen HB, Hirt H, Somssich I, Mattsson O, Mundy J (2005) The MAP kinase substrate MKS1 is a regulator of plant defense responses. EMBO J 24:2579–2589

Asai S, Ohta K, Yoshioka H (2008) MAPK signaling regulates nitric oxide and NADPH oxidase-dependent oxidative bursts in *Nicotiana benthamiana*. Plant Cell 20:1390–1406

Asai S, Ichikawa T, Nomura H, Kobayashi M, Kamiyoshihara Y, Mori H, Kadota Y, Zipfel C, Jones JD, Yoshioka H (2013) The variable domain of a plant calcium-dependent protein kinase (CDPK) confers subcellular localization and substrate recognition for NADPH oxidase. J Biol Chem 288:14332–14340

Balmant KM, Zhang T, Chen S (2016) Protein phosphorylation and redox modification in stomatal guard cells. Front Physiol 7:12

Berriri S, Garcia AV, Frey NFD, Rozhon W, Pateyron S, Leonhardt N, Montillet JL, Leung J, Hirt H, Colcombet J (2012) Constitutively active mitogen-activated protein kinase versions reveal functions of *Arabidopsis* mpk4 in pathogen defense signaling. Plant Cell 24:4281–4293

Brader G, Djamei A, Teige M, Palva ET, Hirt H (2007) The MAP kinase kinase MKK2 affects disease resistance in *Arabidopsis*. Mol Plant Microbe Interact 20:589–596

Brodersen P, Petersen M, Nielsen HB, Zhu SJ, Newman MA, Shokat KM, Rietz S, Parker J, Mundy J (2006) *Arabidopsis* MAP kinase 4 regulates salicylic acid- and jasmonic acid/ethylene-dependent responses via EDS1 and PAD4. Plant J 47:532–546

Cheng SF, Huang YP, Chen LH, Hsu YH, Tsai CH (2013) Chloroplast phosphoglycerate kinase is involved in the targeting of Bamboo mosaic virus to chloroplasts in *Nicotiana benthamiana* plants. Plant Physiol 163:1598–1608

Cui HT, Wang YJ, Xue L, Chu JF, Yan CY, Fu JH, Chen MS, Innes RW, Zhou JM (2010) *Pseudomonas syringae* effector protein AvrB perturbs *Arabidopsis* hormone signaling by activating MAP kinase 4. Cell Host Microbe 7:164–175

Dóczi R, Brader G, Pettkó-Szandtner A, Rajh I, Djamei A, Pitzschke A, Teige M, Hirt H (2007) The *Arabidopsis* mitogen-activated protein kinase kinase MKK3 is upstream of group C mitogen-activated protein kinases and participates in pathogen signaling. Plant Cell 19:3266–3279

Doczi R, Okresz L, Romero AE, Paccanaro A, Bogre L (2012) Exploring the evolutionary path of plant MAPK networks. Trends Plant Sci 17:518–525

Droillard MJ, Boudsocq M, Barbier-Brygoo H, Lauriere C (2004) Involvement of MPK4 in osmotic stress response pathways in cell suspensions and plantlets of *Arabidopsis thaliana*: activation by hypoosmolarity and negative role in hyperosmolarity tolerance. FEBS Lett 574:42–48

Dubiella U, Seybold H, Durian G, Komander E, Lassig R, Witte CP, Schulze WX, Romeis T (2013) Calcium-dependent protein kinase/NADPH oxidase activation circuit is required for rapid defense signal propagation. Proc Natl Acad Sci USA 110:8744–8749

Eng JK, McCormack AL, Yates JR (1994) An approach to correlate tandem mass-spectral data of peptides with amino-acid-sequences in a protein database. J Am Soc Mass Spectrom 5:976–989

Feilner T, Hultschig C, Lee J, Meyer S, Immink RG, Koenig A, Possling A, Seitz H, Beveridge A, Scheel D, Cahill DJ, Lehrach H, Kreutzberger J, Kersten B (2005) High throughput identification of potential *Arabidopsis* mitogen-activated protein kinases substrates. Mol Cell Proteomics 4(10):1558–1568

Furlan G, Nakagami H, Eschen-Lippold L, Jiang X, Majovsky P, Kowarschik K, Hoehenwarter W, Lee J, Trujillo M (2017) Changes in PUB22 ubiquitination modes triggered by mitogen-activated protein kinase3 dampen the immune response. Plant Cell 29:726–745

Goodin MM, Zaitlin D, Naidu RA, Lommel SA (2008) *Nicotiana benthamiana*: its history and future as a model for plant–pathogen interactions. Mol Plant Microbe Interact 21:1015–1026

Hamel LP, Nicole MC, Sritubtim S, Morency MJ, Ellis M, Ehlting J, Beaudoin N, Barbazuk B, Klessig D, Lee J, Martin G, Mundy J, Ohashi Y, Scheel D, Sheen J, Xing T, Zhang S, Seguin A, Ellis BE (2006) Ancient signals: comparative genomics of plant MAPK and MAPKK gene families. Trends Plant Sci 11(4):192–198

Hamel LP, Nicole MC, Duplessis S, Ellis BE (2012) Mitogen-activated protein kinase signaling in plant-interacting fungi: distinct messages from conserved messengers. Plant Cell 24:1327–1351

Hettenhausen C, Baldwin IT, Wu J (2012) Silencing MPK4 in *Nicotiana attenuata* enhances photosynthesis and seed production but compromises abscisic acid-induced stomatal closure and guard cell-mediated resistance to *Pseudomonas syringae* pv tomato DC3000. Plant Physiol 158:759–776

Hoehenwarter W, Thomas M, Nukarinen E, Egelhofer V, Röhrig H, Weckwerth W, Conrath U, Beckers GJM (2013) Identification of novel in vivo MAP kinase substrates in *Arabidopsis thaliana* through use of tandem metal oxide affinity chromatography. Mol Cell Proteomics 12:369–380

Huang X, Liu X, Chen X, Snyder A, Song WY (2013) Members of the XB3 family from diverse plant species induce programmed cell death in *Nicotiana benthamiana*. PLoS ONE 8:9

Katou S, Asakura N, Kojima T, Mitsuhara I, Seo S (2013) Transcriptome analysis of WIPK/SIPK-suppressed plants reveals induction by wounding of disease resistance-related genes prior to the accumulation of salicylic acid. Plant Cell Physiol 54:1005–1015

Kong Q, Qu N, Gao MH, Zhang ZB, Ding XJ, Yang F, Li YZ, Dong OX, Chen S, Li X, Zhang YL (2012) The MEKK1-MKK1/MKK2-MPK4 kinase cascade negatively regulates immunity

mediated by a mitogen-activated protein kinase kinase kinase in *Arabidopsis*. Plant Cell 24:2225–2236

Kosetsu K, Matsunaga S, Nakagami H, Colcombet J, Sasabe M, Soyano T, Takahashi Y, Hirt H, Machida Y (2010) The MAP Kinase MPK4 is required for cytokinesis in *Arabidopsis thaliana*. Plant Cell 22:3778–3790

Lassowskat I, Böttcher C, Eschen-Lippold L, Scheel D, Lee J (2014) Sustained mitogen-activated protein kinase activation reprograms defense metabolism and phosphoprotein profile in *Arabidopsis thaliana*. Front Plant Sci 5:554

Leuzinger K, Dent M, Hurtado J, Stahnke J, Lai H, Zhou X, Chen Q (2013) Efficient agroinfiltration of plants for high-level transient expression of recombinant proteins. JoVE. https://doi.org/10.3791/50521

Li J, Silva-Sanchez C, Zhang T, Chen S, Li H (2015) Phosphoproteomics technologies and applications in plant biology research. Front Plant Sci 6:430

Li S, Wang W, Gao J, Yin K, Wang R, Wang C, Petersen M, Mundy J, Qiu JL (2016) MYB75 phosphorylation by MPK4 is required for light-induced anthocyanin accumulation in *Arabidopsis*. Plant Cell 28:2866–2883

Lian K, Gao F, Sun T, van Wersch R, Ao K, Kong Q, Nitta Y, Wu D, Krysan P, Zhang Y (2018) MKK6 functions in two parallel map kinase cascades in immune signaling. Plant Physiol 178:1284–1295

Liu JZ, Horstman HD, Braun E, Graham MA, Zhang C, Navarre D, Qiu WL, Lee Y, Nettleton D, Hill JH, Whitham SA (2011) Soybean homologs of MPK4 negatively regulate defense responses and positively regulate growth and development. Plant Physiol 157:1363–1378

Liu X, Li J, Xu L, Wang Q, Lou Y (2018) Expressing OsMPK4 impairs plant growth but enhances the resistance of rice to the striped stem borer *Chilo suppressalis*. Int J Mol Sci 19(4):E1182

Ma T, Yoo MJ, Zhang T, Liu L, Koh J, Song WY, Harmon AC, Sha W, Chen S (2018) Characterization of thiol-based redox modifications of *Brassica napus* SNF1-related protein kinase 2.6-2C. FEBS Open Bio 8:628–645

MAPK Group (2002) Mitogen-activated protein kinase cascades in plants: a new nomenclature. Trends Plant Sci 7:301–308

McAlister GC, Nusinow DP, Jedrychowski MP, Wuhr M, Huttlin EL, Erickson BK, Rad R, Haas W, Gygi SP (2014) MultiNotch MS3 enables accurate, sensitive, and multiplexed detection of differential expression across cancer cell line proteomes. Anal Chem 86:7150–7158

Mithoe SC, Menke FL (2018) Regulation of pattern recognition receptor signalling by phosphorylation and ubiquitination. Curr Opin Plant Biol 45:162–170

Norkunas K, Harding R, Dale J, Dugdale B (2018) Improving agroinfiltration-based transient gene expression in *Nicotiana benthamiana*. Plant Methods 14:71

Petersen M, Brodersen P, Naested H, Andreasson E, Lindhart U, Johansen B, Nielsen HB, Lacy M, Austin MJ, Parker JE, Sharma SB, Klessig DF, Martienssen R, Mattsson O, Jensen AB, Mundy J (2000) *Arabidopsis* MAP kinase 4 negatively regulates systemic acquired resistance. Cell 103:1111–1120

Pitzschke A (2015) Modes of MAPK substrate recognition and control. Trends Plant Sci 20:49–55

Pitzschke A, Schikora A, Hirt H (2009a) MAPK cascade signalling networks in plant defence. Curr Opin Plant Biol 12:421–426

Pitzschke A, Djamei A, Bitton F, Hirt H (2009b) A major role of the MEKK1-MKK1/2-MPK4 pathway in ROS signalling. Mol Plant 2:120–137

Popescu SC, Popescu GV, Bachan S, Zhang Z, Gerstein M, Snyder M, Dinesh-Kumar SP (2009) MAPK target networks in *Arabidopsis thaliana* revealed using functional protein microarrays. Genes Dev 23:80–92

Qi T, Seong K, Thomazella DPT, Kim JR, Pham J, Seo E, Cho MJ, Schultink A, Staskawicz BJ (2018) NRG1 functions downstream of EDS1 to regulate TIR-NLR-mediated plant immunity in *Nicotiana benthamiana*. Proc Natl Acad Sci USA 115:E10979–E10987

Qiu JL, Fiil BK, Petersen K, Nielsen HB, Botanga CJ, Thorgrimsen S, Palma K, Suarez-Rodriguez MC, Sandbech-Clausen S, Lichota J, Brodersen P, Grasser KD, Mattsson O, Glazebrook J, Mundy J, Petersen M (2008) Arabidopsis MAP kinase 4 regulates gene expression through transcription factor release in the nucleus. EMBO J 27(16):2214–2221

Rayapuram N, Bigeard J, Alhoraibi H, Bonhomme L, Hesse AM, Vinh J, Hirt H, Pflieger D (2018) Quantitative phosphoproteomic analysis reveals shared and specific targets of *Arabidopsis* mitogen-activated protein kinases (MAPKs) MPK3, MPK4, and MPK6. Mol Cell Proteomics 17:61–80

Ren D, Yang KY, Li GJ, Liu Y, Zhang S (2006) Activation of Ntf4, a tobacco mitogen-activated protein kinase, during plant defense response and its involvement in hypersensitive response-like cell death. Plant Physiol 141:1482–1493

Singh R, Lee MO, Lee JE, Choi J, Park JH, Kim EH, Yoo RH, Cho JI, Jeon JS, Rakwal R, Agrawal GK, Moon JS, Jwa NS (2012) Rice mitogen-activated protein kinase interactome analysis using the yeast two-hybrid system. Plant Physiol 160:477–487

Su J, Yang L, Zhu Q, Wu H, He Y, Liu Y, Xu J, Jiang D, Zhang S (2018) Active photosynthetic inhibition mediated by MPK3/MPK6 is critical to effector-triggered immunity. PLoS Biol 16:e2004122

Takahashi Y, Nasir KH, Ito A, Kanzaki H, Matsumura H, Saitoh H, Fujisawa S, Kamoun S, Terauchi R (2007) A high-throughput screen of cell-death-inducing factors in *Nicotiana benthamiana* identifies a novel MAPKK that mediates INF1-induced cell death signaling and non-host resistance to *Pseudomonas cichorii*. Plant J 49:1030–1040

Tian T, Liu Y, Yan HY, You Q, Yi X, Du Z, Xu WY, Su Z (2017) agriGO v2.0: a GO analysis toolkit for the agricultural community, 2017 update. Nucleic Acids Res 45:W122–W129

Umezawa T, Sugiyama N, Takahashi F, Anderson JC, Ishihama Y, Peck SC, Shinozaki K (2013) Genetics and phosphoproteomics reveal a protein phosphorylation network in the abscisic acid signaling pathway in *Arabidopsis thaliana*. Sci Signal 6:rs8

Wang Z, Mao H, Dong C, Ji R, Cai L, Fu H, Liu S (2009) Overexpression of *Brassica napus* MPK4 enhances resistance to *Sclerotinia sclerotiorum* in oilseed rape. Mol Plant Microbe Interact 22:235–244

Wang P, Xue L, Batelli G, Lee S, Hou YJ, Van Oosten MJ, Zhang H, Tao WA, Zhu JK (2013) Quantitative phosphoproteomics identifies SnRK2 protein kinase substrates and reveals the effectors of abscisic acid action. Proc Natl Acad Sci USA 110(27):11205–11210

Wang Y, Weide R, Govers F, Bouwmeester K (2015) L-type lectin receptor kinases in *Nicotiana benthamiana* and tomato and their role in *Phytophthora* resistance. J Exp Bot 66:6731–6743

Wang Y, Xu Y, Sun Y, Wang H, Qi J, Wan B, Ye W, Lin Y, Shao Y, Dong S, Tyler BM, Wang Y (2018) Leucine-rich repeat receptor-like gene screen reveals that *Nicotiana* RXEG1 regulates glycoside hydrolase 12 MAMP detection. Nat Commun 9:594

Xie G, Kato H, Imai R (2012) Biochemical identification of the OsMKK6-OsMPK3 signalling pathway for chilling stress tolerance in rice. Biochem J 443:95–102

Xu J, Zhang S (2015) Mitogen-activated protein kinase cascades in signaling plant growth and development. Trends Plant Sci 20:56–64

Yamada K, Yamaguchi K, Shirakawa T, Nakagami H, Mine A, Ishikawa K, Fujiwara M, Narusaka M, Narusaka Y, Ichimura K, Kobayashi Y, Matsui H, Nomura Y, Nomoto M, Tada Y, Fukao Y, Fukamizo T, Tsuda K, Shirasu K, Shibuya N, Kawasaki T (2016)

The *Arabidopsis* CERK1-associated kinase PBL27 connects chitin perception to MAPK activation. EMBO J 35:2468–2483

Zhang T, Chen S, Harmon AC (2014) Protein phosphorylation in stomatal movement. Plant Signal Behav 9:e972845

Zhang T, Zhu MM, Song WY, Harmon AC, Chen S (2015) Oxidation and phosphorylation of MAP kinase 4 cause protein aggregation. Biochim Biophys Acta Proteins Proteomics 1854:156–165

Zhang T, Chen S, Harmon AC (2016) Protein–protein interactions in plant mitogen-activated protein kinase cascades. J Exp Bot 67:607–618

Zhang T, Schneider JD, Zhu N, Chen S (2017) Identification of MAPK substrates using quantitative phosphoproteomics. Methods Mol Biol 1578:133–142

Zhang M, Su J, Zhang Y, Xu J, Zhang S (2018a) Conveying endogenous and exogenous signals: MAPK cascades in plant growth and defense. Curr Opin Plant Biol 45:1–10

Zhang T, Meng L, Kong W, Yin Z, Wang Y, Schneider JD, Chen S (2018b) Quantitative proteomics reveals a role of JAZ7 in plant defense response to *Pseudomonas syringae* DC3000. J Proteomics 175:114–126

Zhang T, Schneider JD, Lin C, Geng S, Ma T, Lawrence SR, Dufresne CP, Harmon AC, Chen S (2019) MPK4 phosphorylation dynamics and interacting proteins in plant immunity. J Proteome Res 18(3):826–840

Zhao X, Kim Y, Park G, Xu JR (2005) A mitogen-activated protein kinase cascade regulating infection-related morphogenesis in *Magnaporthe grisea*. Plant Cell 17:1317–1329

Zhu M, Zhang T, Ji W, Silva-Sanchez C, Song WY, Assmann SM, Harmon AC, Chen S (2017) Redox regulation of a guard cell SNF1-related protein kinase in *Brassica napus*, an oilseed crop. Biochem J 474:2585–2599

Zipfel C, Kunze G, Chinchilla D, Caniard A, Jones JD, Boller T, Felix G (2006) Perception of the bacterial PAMP EF-Tu by the receptor EFR restricts *Agrobacterium*-mediated transformation. Cell 125:749–760

Zulawski M, Schulze G, Braginets R, Hartmann S, Schulze WX (2014) The *Arabidopsis* Kinome: phylogeny and evolutionary insights into functional diversification. BMC Genomics 15:548